

## Images of the Phonon Propagation across Twist-Bonded Crystals

M. Msall,<sup>1</sup> W. Dietsche,<sup>2</sup> K.-J. Friedland,<sup>3</sup> and Q.-Y. Tong<sup>4,\*</sup>

<sup>1</sup>*Department of Physics, Bowdoin College, Brunswick, Maine 04011*

<sup>2</sup>*Max-Planck-Institut für Festkörperforschung, Postfach 800665, D70506 Stuttgart, Germany*

<sup>3</sup>*Paul-Drude-Institut für Festkörperelektronik, Hausvogteiplatz 5-7, D11017 Berlin, Germany*

<sup>4</sup>*Research Triangle Institute, Research Triangle Park, North Carolina 27709*

(Received 30 November 1999)

We investigate identical but twist-bonded crystals using phonon imaging techniques. As in homogeneous crystals, very anisotropic flux patterns are observed. However, the shape of the pattern depends dramatically on the respective twist angle. The observed phonon images in wafer bonded GaAs/GaAs and Si/Si samples are essentially consistent with the predictions of the acoustic mismatch model for defect-free interfaces, with the exception of GaAs wafers twist bonded at a 45° angle where modes with large shear stress are missing, which indicates strong dislocation scattering.

PACS numbers: 66.70.+f, 61.50.Lt

The dramatic anisotropy of the ballistic propagation of acoustic phonons is easily visualized using phonon imaging techniques [1]. The concentration of phonon flux emanating from a pointlike source along a few crystalline directions (an effect known as phonon focusing) is a natural consequence of the acoustic anisotropy of crystalline materials. Homogeneous materials have mainly been studied by this technique [2,3] because ever present contaminants and defects at surfaces and interfaces scatter phonons very effectively, making elastic transmission between two different materials virtually impossible [4]. Exceptions are the studies of domain wall boundaries in KDP [2] and interfaces prepared by epitaxial growth with molecular-beam-epitaxy techniques [3]. Surface contaminants are also the source of the Kapitza anomaly, i.e., the anomalously large phonon transfer into liquid helium at crystalline surfaces [5].

The technique of “wafer direct bonding” [6] creates bonds between two crystals which are essentially free of phonon-scattering defects. The acoustic properties of these interfaces are amenable to investigations using phonon imaging [7]. In this Letter, we investigate the novel case where crystals are twisted with respect to each other prior to bonding and address the question, “Do new types of phonon focusing exist because of the change in crystalline anisotropy on opposite sides of the bond”?

At a perfect bond, Snell’s law requires conservation of phonon frequency and of the wave vector component parallel to the plane of the interface. In general, the interface acts trirefringent on the phonons, producing as many as three reflected and three transmitted modes which will affect the phonon focusing patterns in the twist-bonded samples.

Previously published phonon images of 0° twist-bonded GaAs show phonon focusing features in good agreement with those of single crystal GaAs [7]. This indicates that many of the phonon trajectories are essentially unaffected by the bonded interface and that a significant fraction of the detected phonons is not scattered at the interface.

Scattering would mean that the phonon momenta were randomized after passing the interface rather than being determined by Snell’s law.

The trajectories must be affected by the interface, however, if the two media are acoustically different, as they are in bonded samples with nonzero twist angles. In this case, the incident phonon mode may convert into three transmitted and three reflected modes which have the same parallel momentum and the same frequency as the incident phonon. The relative weights of the transmitted and reflected modes can be determined by the acoustic mismatch theory. This requires, firstly, that the sum of the three phonon amplitude components of the six outgoing modes is equal to the amplitude of the incident phonon and, secondly, that the sums of the three stress components acting perpendicular to the interface are conserved as well. This leads to six equations from which the amplitudes of the reflected and transmitted phonons are uniquely determined.

The expected changes in the phonon images at varying twist angle can be determined by a computer program that calculates the group velocity for an isotropic distribution of phonon wave vectors [1]. Phonon trajectories for these wave vectors (for all three possible modes) are then calculated and the points of intersection with the bonded interface are marked. The transmitted and reflected phonon modes, as well as their amplitudes, are determined by using the expressions published by Kinder and Weiss [8] based on the amplitude and stress continuity conditions outlined above. Once the new modes and their respective group velocities are determined, new phonon trajectories for each possible transmitted wave are calculated. When a phonon trajectory intersects the detection surface it is recorded by a count proportional to its respective power flux. These data can be displayed so that the color at each point on the simulated image indicates the power of the phonon flux arriving at that point.

Simulated images for twist-bonded (100) Si and GaAs wafers are displayed in Figs. 1(b), 2(b), and 3(b). These images are considerably different from the well-known

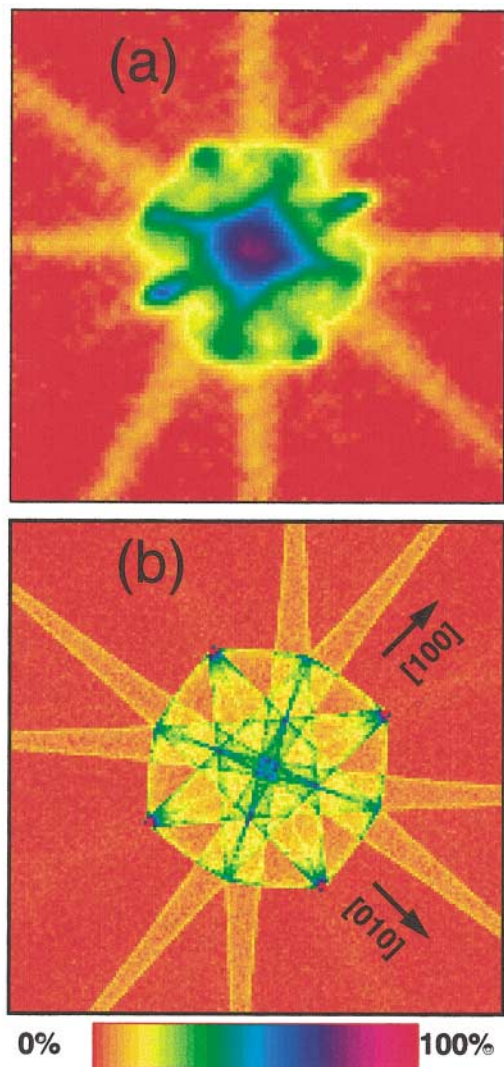


FIG. 1 (color). (a) Experimentally observed phonon focusing image in twist-bonded Si with a twist angle of  $40^\circ$ . Each of the two bonded crystals are 3 mm thick, the length of the image sides correspond to 2 mm. (b) Simulated image for the same experimental condition. The arrows indicate the crystal orientation relative to the phonon source. The sample normal points in the  $[001]$  direction. The second crystal is twisted in the clockwise direction. At the bottom is the color table used in this and the following figures. The phonon intensities are normalized to the maximum value of the respective image.

images of homogeneous single crystals [1] but still show the sharp structures typical of phonon focusing. The new focusing patterns also depend upon the relative thicknesses of the two bonded pieces. For example, simulations show that the double lines of high intensity seen in all of these three images may collapse into a single line at a certain critical thickness ratio and will disappear altogether if that ratio is exceeded. This ability to produce concentrations of phonon flux at certain points suggests novel applications of bonded interfaces as “phonon lenses”.

It is even more interesting if the novel focusing patterns can actually be observed experimentally. Networks of dis-

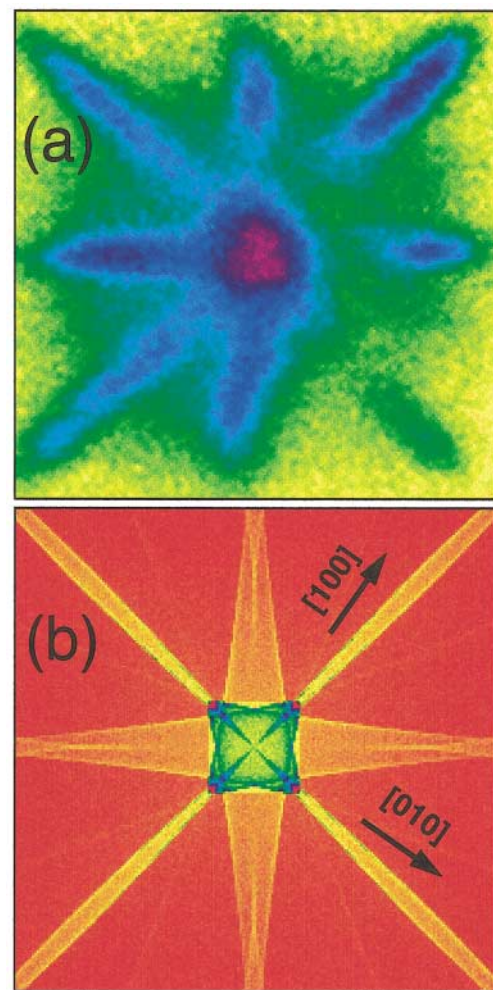


FIG. 2 (color). Experimentally observed (a) and simulated (b) phonon image for GaAs crystals bonded at  $20^\circ$ . The thicknesses of the bonded wafers are  $300\ \mu\text{m}$  each, the image sides correspond to 1 mm. The fine-structures of the simulated image cannot be observed due to both the reduced spatial resolution in the thinner wafer and the residual phonon scattering in the GaAs. The arrows in (b) refer to the orientation of the first of the two bonded crystals. Note that the structures do not coincide directly with the crystal orientations which are marked by the arrows.

locations form at the interfaces of twist-bonded crystal to accommodate the strains of the lattice mismatch [6] and will possibly affect phonon transmission. Dislocations in the bulk of single crystals are known to scatter phonons rather effectively [9]. On the other hand, the same dislocations may trap the residual impurities which are detrimental to phonons at standard free interfaces.

In this investigation, we use both bonded GaAs/GaAs and Si/Si wafers. The GaAs samples are constructed from pieces of standard undoped  $400\ \mu\text{m}$  (001) GaAs wafers, bonded after etching with hydrogen peroxide followed by a heat treatment at  $700^\circ\text{C}$  for 30 min [7]. The samples were prepared in two similarly processed batches, with varying twist angles about the  $[001]$  axis of  $0^\circ$ ,  $20^\circ$ ,  $30^\circ$ , and  $45^\circ$ . The exterior surfaces were then mechanically polished and

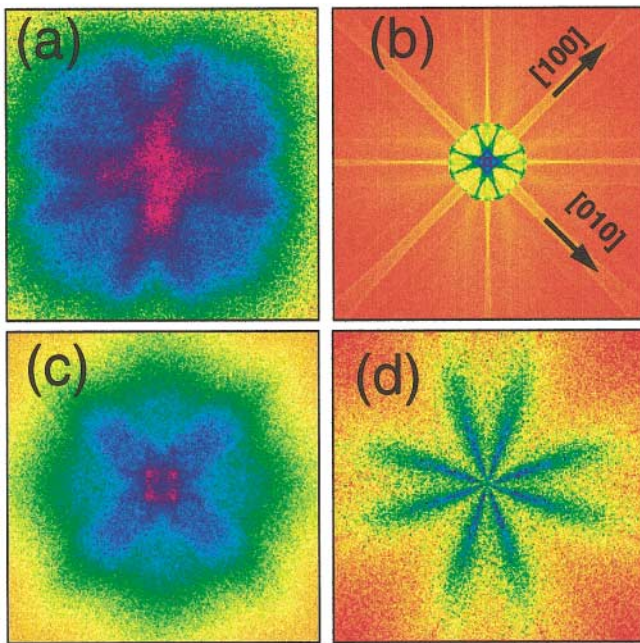


FIG. 3 (color). (a) Experimentally observed image for two GaAs crystals bonded at  $45^\circ$ , (b) Simulated image using acoustical boundary conditions, (c) Simulated phonon image assuming a complete randomization of the momenta at the interface, (d) Simulations showing only the FT-FT contribution to the simulated image. The thicknesses of the wafers are  $300\ \mu\text{m}$  and  $360\ \mu\text{m}$ , respectively. The image sides correspond to 1 mm. The orientation of the crystals is marked in (b).

chemically etched, reducing the final (total) thickness to about  $600\ \mu\text{m}$ .

The Si/Si bonding is difficult because of our choice of thick (3 mm) Si substrates (which form better resolved phonon images) for bonding and because of the tendency of clean Si surfaces to oxidize. Both hydrophobic and hydrophilic bondings were tested. Hydrophobic bonding, in which the surface is protected from oxidation by hydrogen termination, often leads to the formation of tiny voids at the interface causing blurred phonon images which will not be shown here. Hydrophilic bonding, in which the natural surface oxides are not removed, has a localized impurity layer ( $\text{SiO}_x$ ) at the interface but fewer voids. This leads to much better phonon images. The bonded samples were annealed at  $1050\ ^\circ\text{C}$  for 3 h. A hydrophilic bonded sample with a twist angle about the  $[001]$  axis of  $40^\circ$ , with a final total sample thickness of 6.0 mm, is used.

We measure the phonon propagation through the samples using the techniques of phonon imaging [1]. An Al film directly evaporated on the sample surface is photoexcited by 10 ns pulses of an  $\text{Ar}^+$  laser or a 690 nm diode laser. The laser energy is focused to a spot of about  $10\ \mu\text{m}$  diameter) which is heated to typically 5 K [10] and radiates acoustical phonons into the crystal. These phonons have an approximate Planckian frequency distribution with typical frequencies of several 100 GHz corresponding to wavelengths of approximately 10 nm

and are able to travel macroscopic distances ballistically. Phonon arrivals on the opposite surface are measured using a superconducting Al bolometer (active area about  $10\ \mu\text{m}$  in diameter). The angular dependence of the phonon propagation is measured by raster scanning the mirrors that position the laser on the sample surface. In order to bias the bolometer near its superconducting transition and to minimize background thermal vibrations, the sample is immersed in liquid helium near 1.5 K. The detected phonon signal from each laser excitation point is averaged over thousands of laser pulses using an EG&G 9825 digital signal averaging card.

The experimental image of  $40^\circ$  hydrophilically twist-bonded Si shows indeed sharp phonon focusing features [Fig. 1(a)] which coincides nearly perfectly with our theoretical prediction [Fig. 1(b)]. The complex pattern of the central star-shape is due to slow transverse (ST) polarized phonons that are transmitted into new ST phonon modes at the interface. The agreement between experiment and simulation shows that the oxide layer which is present on hydrophilic bonding is not harmful to the phonon transmission as expected on the acoustic mismatch theory.

The experimental image of a GaAs sample with a  $20^\circ$  twist angle shows focusing structures that are less sharp than in the Si sample due to its smaller total thickness  $600\ \mu\text{m}$ . Bulk phonon scattering also contributes to a blurring of the images. Nevertheless, focusing structures in reasonable agreement with the theoretical prediction are clearly observed, indicating that acoustic transmission exists. The features running perpendicular and horizontal relative to the figure orientation are due to the transitions of fast transverse (FT) into other FT phonons. The ones along the diagonals are caused by ST to ST transitions. The two types of ridges are of similar strengths which is expected if one integrates the theoretical intensities over an area corresponding to the experimentally achieved resolution ( $50\ \mu\text{m}$ ). A similarly good focusing pattern (not shown) is also observed for a  $30^\circ$  twist-bonded GaAs sample which agrees similarly well with the simulated one.

Finally, we consider a  $45^\circ$  twist angle. Because our twist axis is a fourfold symmetry axis of single crystal GaAs, we expect an eightfold symmetric image from  $45^\circ$  twist-bonded, equal-thickness pieces. Under our experimental condition this symmetry is broken because the bonded pieces are not of equal thickness (actual thicknesses were  $300\ \mu\text{m}$  before the bond and  $360\ \mu\text{m}$  after the bond). The experimental image [Fig. 3(a)] shows clear focusing structures, which should indicate the applicability of Snell's law. However, the observed structures do not coincide at all with the features of the simulated image [Fig. 3(b)]. This is a very surprising result.

In an attempt to understand this result, we first tried a completely different simulation that assumed complete randomization of the phonon momenta, i.e., strong scattering, at the interface [Fig. 3(c)]. This image shows features which are much less sharp than the acoustic simulation

[Fig. 3(b)] and does not reproduce the features of the experimental image [Fig. 3(a)].

Next, we repeated simulations of the acoustic transmission, but binned the phonons separately according to the type of mode conversion that occurred at the interface. Incoming and outgoing modes were sorted according to the absolute values of their wave vectors. By using this sorting, we find that our theoretical images are dominated by incoming ST modes that are converted into outgoing ST modes. If we consider instead the incoming FT modes that are converted into outgoing FT modes [Fig. 3(d)], then we find focusing patterns that closely resemble those seen in the experimental images. These FT modes are present in the complete theoretical image [Fig. 3(b)] but are too faint in comparison to the dominant ST mode to be seen. This suggests that the normal occupancy ratio of the two transverse modes is strongly modified during transmission through the interface.

What could cause such an imbalance of the transmitted phonon modes? A likely origin is dislocations that form at the bond interface to accommodate lattice mismatch. It is known that the strength of phonon scattering from dislocations is proportional to  $\mathbf{b}\sigma_0$ , where  $\mathbf{b}$  is the Burgers vector and  $\sigma_0$  is the shear stress acting on the dislocation [11]. This was experimentally verified by the observation that phonons with the appropriate shear component are strongly scattered in LiF containing many dislocations [9]. It is not entirely clear how this model should be adapted for the twist-bond case. However, if we divide the amplitudes of the outgoing phonon modes in our simulations by the sum of squares of the three shear components then the relative weight of the FT modes becomes comparable to that of the ST modes. This indicates that the modes which are missing in the experiment in Fig. 3 are indeed those with the larger shear. We have not yet succeeded in producing simulated images that perfectly reproduce the experimental focusing patterns, but our preliminary simulations demonstrate the importance of the shear stresses for phonon scattering at the  $45^\circ$  bonded interface.

Dislocations are, of course, present at all twist-bonded interfaces and it is not obvious why they have such dramatic impact on phonon propagation at a single twist-bond angle. In the special case of  $45^\circ$ , however, TEM studies on bonded GaAs wafers reveal only pure edge-type dislocations at the interface, whereas at other angles such dislocation structures are not sufficient to accommodate the misorientations [12]. At small angles, pure screw dislocations only are needed. It appears quite possible that the increased density of edge dislocations leads to strong scattering of phonon modes with a large shear component.

In conclusion, we observe phonon focusing structures in twist-bonded crystals that verify the appropriateness of the acoustic mismatch model in describing real interfaces. Sharp phonon focusing features exist despite the birefringent refraction. Unlike the homogeneous case, where the term “phonon focusing” does not imply geometrical bending of particle paths, our observations show a substantial change of direction of phonon paths at an interface. This effect can be exploited in a variety of situations including “real” focusing, where phonon control is desirable. Further experimental and theoretical studies of the variations in true phonon focusing as a function of interface and substrate parameters will allow increasingly refined control of this new phonon optics.

We thank S. Kronmüller for helping with the phonon technology. A. Klimashov and A. Riedel assisted with the bonding of the GaAs wafers. We are grateful to K. v.Klitzing, and H.-J. Queisser for their constant interest and encouragement. The help of U. Gösele in initiating the collaboration between Q.-Y. Tong and the other authors is gratefully acknowledged.

---

\*Also at School of Engineering, Duke University, Durham, NC 27708.

- [1] J. P. Wolfe, *Imaging Phonons: Acoustic Wave Propagation in Solids* (Cambridge University Press, Cambridge, England, 1998).
- [2] M. A. Weilert, M. E. Msall, A. C. Anderson, and J. P. Wolfe, *Phys. Rev. Lett.* **71**, 735 (1993).
- [3] S. Tamura, D. C. Hurley, and J. P. Wolfe, *Phys. Rev. B* **38**, 1427 (1988).
- [4] See, for example, the review by E. T. Swartz and R. O. Pohl [*Rev. Mod. Phys.* **61**, 605 (1989)].
- [5] J. Weber, W. Sandmann, W. Dietsche, and H. Kinder, *Phys. Rev. Lett.* **40**, 1469 (1978).
- [6] For a recent review see U. Gösele *et al.*, *J. Vac. Sci. Technol. A* **17**, 1145 (1999).
- [7] M. E. Msall, A. Klimashov, S. Kronmüller, H. Kostial, W. Dietsche, and K. Friedland, *Appl. Phys. Lett.* **74**, 821 (1999).
- [8] H. Kinder and K. Weiss, *J. Phys. Condens. Matter* **5**, 2063 (1993).
- [9] G. A. Northrop, E. J. Cotts, A. C. Anderson, and J. P. Wolfe, *Phys. Rev. B* **27**, 6395 (1983).
- [10] F. Rösch and O. Weis, *Z. Phys. B* **46**, 33 (1977).
- [11] G. A. Kneezel and A. V. Granato, *Phys. Rev. B* **25**, 2851 (1982).
- [12] A. Trampert, K. Friedland, and K. Ploog (to be published).